Pharmaceutical Sciences, 2024, 30(1), 109-115
doi:10.34172/PS.2023.2
https://ps.tbzmed.ac.ir/

Research Article

Experimental, Modeling and Molecular Dynamics Simulation of Codeine Phosphate Dissolution in N-Methyl-2-pyrrolidone + Ethanol

Homa Rezaei[1,2], Martin Kuentz[3], Hongkun Zhao[4], Elaheh Rahimpour[2,5*], Abolghasem Jouyban[2,6]

[1]*Student Research Committee, Faculty of Pharmacy, Tabriz University of Medical Sciences, Tabriz, Iran.*
[2]*Pharmaceutical Analysis Research Center and Faculty of Pharmacy, Tabriz University of Medical Sciences, Tabriz, Iran.*
[3]*Institute of Pharma Technology, University of Applied Sciences and Arts Northwestern Switzerland, Hofackerstr. 30, 4132 Muttenz, Switzerland.*
[4]*College of Chemistry and Chemical Engineering, YangZhou University, YangZhou, Jiangsu 225002, People's Republic of China.*
[5]*Food and Drug Safety Research Center, Tabriz University of Medical Sciences, Tabriz, Iran.*
[6]*Faculty of Pharmacy, Near East University, PO BOX: 99138 Nicosia, North Cyprus, Mersin 10, Turkey.*

Article Info

Article History:
Received: 28 Nov 2022
Accepted: 5 Jan 2023
ePublished: 20 Sep 2023

Keywords:
-Binary solvent mixture
-Codeine phosphate
-Cosolvency equations
-Solubility

Abstract

Background: There is only limited data for solubility of codeine phosphate in binary systems available, which comes with uncertainties about the prediction accuracy of common thermodynamic models.

Methods: This study investigated the codeine phosphate dissolution in N-methyl-2-pyrrolidone (NMP) and ethanol system using shake-flask method and mathematically described generated data by different thermodynamic models. The density as another property was also determined and fitted to results of the Jouyban-Acree equation. The mean relative deviations were obtained to confirm the model's accuracy. Moreover, ΔH^o, ΔS^o, and ΔG^o of the dissolution of codeine phosphate in the NMP and ethanol system were calculated using the desired equations at T_{hm}.

Results: The dissolution process of codeine phosphate was identified as endotherm, the solubility in the binary mixtures was best at higher mass fractions of NMP and finally, the model predictions were deemed as excellent based on a mean relative deviation that was generally below eight percent.

Conclusion: The results of this study could expand the available solubility database for codeine phosphate.

Introduction

Codeine phosphate (Figure 1) is the opioid drug with a weak capability of binding to μ-opioid receptors. It is a compound with different clinical effects as used in pain relief, or treatment of cough and diarrhea, whereby a fraction of the dose is converted to morphine.[1,2] Codeine is present in unripe seed capsules of the poppy plant.[1] Therefore, its extraction from natural products plays a crucial role in the pharmaceutical and chemical industries. Liquid-liquid extraction, also known as solvent partitioning technique, is a critical separation processes in chemical engineering in which substances will separate according to solubility in two different or immiscible solvents.[2] The ability to select the best solvent from a wide range of solvents and the low cost of relevant devices are the most important advantages of this process.[2] Therefore, the knowledge of solubility is extremely important for the selection of the best solvent/antisolvent system. Apart from extraction purposes, there are further galenical processes that harness co-solvent mixtures as intermediate bulk solutions and, in this context, it is usually the maximum drug solubility that is targeted for further processing to obtain the final dosage form, for example, by a microprecipitation or spray-drying process.

Understanding of the respective drug dissolution mechanisms is considered as crucial in chemical engineering and the pharmaceutical sciences and therefore it is vital to extend the available solubility database of pharmaceuticals for its broad spectrum usage in pharmaceutical and chemical industries.[3,4] Codeine usually exists in salt form in the market. So far, only limited studies were available for the experimental solubility of codeine phosphate. The published studies include investigation of codeine phosphate in neat solvents of water and ethanol, binary organic solvents of N-methyl-2-pyrrolidone (NMP) + 2-propanol and carbitol + 2-propanol which are our previous efforts. However, there appears to be no solubility value for codeine phosphate in NMP + ethanol in database. NMP is a polar aprotic and stable solvent with high usage in the pharmaceutical industry.[5-7] Furthermore, ethanol is

*Corresponding Author: Elaheh Rahimpour, E-mail: rahimpour_e@yahoo.com

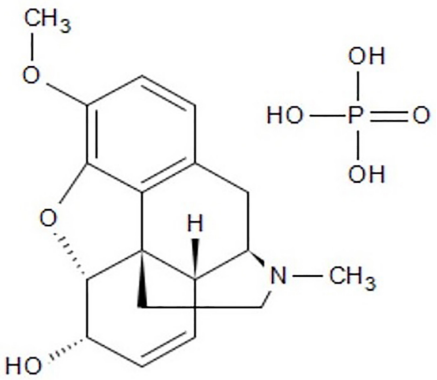

Figure 1. Molecular structure of codeine phosphate.

a widely used solvent/cosolvent with many applications in drug extraction, purification, microparticles production and tablet polymeric coating.[8]

Herein we want to (i) report some physico-chemical properties of codeine phosphate in NMP and ethanol system at five temperatures; (ii) mathematical representation of data with the well-known models; and (iii) report ΔH^o, ΔS^o, and ΔG^o for the desired solute in NMP and ethanol system.

Methods

Materials

Codeine phosphate (0.997, Daana Pharmaceutical Company, Iran), ethanol (0.995, Scharlau Chemie, Spain) and NMP (0.980, Merck, Germany), were used herein. Ethanol (0.935, Jahan Alcohol Teb, Arak, Iran) in combination with deionized water with conductivity of <3 μS cm^{-1} was utilized for dilution.

Solubility determination

A simple shake-flask technique[9] was utilized in this work. Eleven glass vials were filled with 10 g ethanol and NMP solvents in various NMP mass fraction ratios of 0.0 to 1.0 with interval of 0.1. Codeine phosphate powder in excess amount was dispensed into the glasses containing the above solutions. Then, they entered in an incubator (Kimia Idea Pardaz Azerbaijan (KIPA.co), Iran) on a shaker (Behdad, Iran) at the adjusted temperature in the range of 293.2–313.2 K (uncertainty of 0.2 K) at ambient humidity and pressure for of 48 h. Temperature was adjusted into a big incubator which the shaker was entered into it and all solubility dilution procedures were performed in it using special vents for hands. A schematic picture of the incubator was given in Figure S1 in Supplementary Data. Subsequently at the end of the equilibration time, the saturated solutions were centrifuged by 6000 rpm and the supernatant solution was separated. These solutions were diluted with ethanol: water mixture (30:70) in the right proportion and analyzed at 285 nm using a UV–Vis spectrophotometer (Cecil BioAquarius CE 7250, UK). Absorbance of the solutions were recorded and the concentrations were calculated using the interpolation from a previously constructed calibration curve.

A pycnometer with 5 mL volume was used for density determination. Digital balance had been placed in closet possible place to the incubator. Solutions and pycnometer reach the temperature equilibration into the mentioned incubator and the weight reading was performed immediately after equilibration out of incubator. All measurements were performed three times and mean of them were reported as a main data in this work.

Statistical models

Solubility data was fitted to the van't Hoff, the mixture response surface (MRS), the Jouyban-Acree, the Jouyban-Acree-van't Hoff and λh equations that present in Eqs. (1) to (5):[10-12]

$$\ln x = A + \frac{B}{T} \qquad \text{Eq. (1)}$$

Here A and B are the model parameters.

$$\ln x_m = \beta_1 w'_1 + \beta_2 w'_2 + \beta_3 \left(\frac{1}{w'_1}\right) + \beta_4 \left(\frac{1}{w'_2}\right) + \beta_5 w'_1 w'_2 \qquad \text{Eq. (2)}$$

Here β_1-β_5 are equation parameters and w'_1 and w'_2 are calculated by using w'_1=0.96 w_1 + 0.02 and w'_2=0.96 w_2 + 0.02. w_1 and w_2 are the mass fractions of solvents 1 and 2 in the absence of solute. x_m is the solubility value in the mixtures.

$$\ln x_{m,T} = w_1 \ln x_{1,T} + w_2 \ln x_{2,T} + \frac{w_1 w_2}{T} \sum_{i=0}^{2} J_i .(w_1 - w_2)^i \qquad \text{Eq. (3)}$$

$$\ln x_{m,T} = w_1 (A_1 + \frac{B_1}{T}) + w_2 (A_2 + \frac{B_2}{T}) + \frac{w_1 w_2}{T} \sum_{i=0}^{2} J_i .(w_1 - w_2)^i \qquad \text{Eq. (4)}$$

Here $x_{1,T}$ and $x_{2,T}$ are the solute solubility (in mole fraction unit) in the mono solvents 1 and 2, $x_{m,T}$ is the drug solubility in the mixtures at temperature T, and J_i terms are the model parameters obtained by linear regression.

$$\ln\left[1 + \frac{\lambda(1-x)}{x}\right] = \lambda h \left[\frac{1}{T} - \frac{1}{T_m}\right] \qquad \text{Eq. (5)}$$

in which λ and h are the equation parameters obtained by simple nonlinear analysis.

Eq (6) is used for investigation of the deviation of back-calculated data with measured data and called mean relative deviation (*MRD* %):

$$\%MRD = \frac{100}{N} \sum \left(\frac{|Calculated\ Value - Observed\ Value|}{Observed\ Value} \right) \qquad \text{Eq. (6)}$$

N is data points number.

Thermodynamic studies

In this section, the Gibbs and van't Hoff equations were utilized. The modified van't Hoff model can be written as:

$$\frac{\delta \ln x}{\delta\left(\frac{1}{T}-\frac{T}{T_{hm}}\right)_p}=-\frac{\Delta H^{\circ}}{R} \qquad \text{Eq. (7)}$$

R is the ideal gas constant, T_{hm} is obtained from the Eq. 8 :

$$T_{hm}=n/\sum_{i=1}^{n}(1/T) \qquad \text{Eq. (8)}$$

n is the temperature number. ΔH^o and ΔG^o are found from the slope and the intercept of the modified van't Hoff curve,[13] and ΔS^o were obtained by the Gibbs equation. Relative contributions of enthalpy and entropy for the investigated system were found from Eqs. 9 and 10.

$$\zeta_H=\frac{\left|\Delta H^0\right|}{\left(\left|\Delta H^0\right|+\left|T\,\Delta S^0\right|\right)} \qquad \text{Eq. (9)}$$

$$\zeta_{TS}=\frac{\left|T\,\Delta S^0\right|}{\left(\left|\Delta H^0\right|+\left|T\,\Delta S^0\right|\right)} \qquad \text{Eq. (10)}$$

Molecular dynamics simulation

The YASARA software v. 20.12.24 (YASARA Biosciences GmbH, Vienna, Austria)[14] was used for molecular dynamics (MD) simulation. An AMBER 14 type force field was selected together with a cut-off of 8 Å for long-range molecular interactions using a particle mesh Ewald approach[15] for electrostatic forces. Molecular charges were calculated by a semi-empirical quantum chemical method, i.e., AM1-BCC.[16] A cubic simulation cell of 100 Å side length was employed by an isothermal-isobaric ensemble (NPT) at 298.2 K and 1.0 bar. The solvents molecules ethanol and NMP were simulated in equal numbers together with three molecules of codeine phosphate in the simulation cell. After steepest descent and simulated annealing minimizations to eliminate clashes, the simulation is run for 5 ns by utilizing a time step of 2x 1ns for integration of the equations of motion.

Results and Discussion

Profile for solubility and data modeling

Solubility values are reported at Table 1 along with the standard deviation of replication. As can be seen, the solubility increased by rising NMP concentration and maximum value was yielded at neat NMP. Furthermore, the solubility values show a direct relation with temperature. Minimum value in solubility pattern was in pure ethanol at 293.2 K and maximum one is d for pure NMP at high investigated temperature. Figure 2 shows a comparison between the current investigation systems for codeine phosphate with those reported in our previous studies. As can be seen, the best solubilization effect is obtained for NMP + ethanol system at 298.2 K.

Data was fitted to selected the well-known cosolvency equations and their parameters and *MRDs*% of data were summarized in Tables 2-5. MRS predict solubility at mixture in isothermal condition with *MRDs*% of 3.7% and the Jouyban-Acree and the Jouyban-Acree-van't Hoff equations predict data at all conditions depended to temperature and mass fraction with *MRDs*% 7.6% and 8.0%, respectively. The van't Hoff and λh equations as two equations for prediction at each mixture composition at different temperatures showed *MRDs*% of 2.0 and 3.4%. As can be seen, *MRDs*% are within acceptable error ranges and lie in uncertainty ranges of an experimental.

The densities were measured and correlated with the Jouyban-Acree equation. Trained equation (Eq. 11) for density amounts is:

$$\ln \rho_{m,T}=w_1.\ln \rho_{1,T}+w_2.\ln \rho_{2,T}+14.232\frac{w_1 w_2}{T} \qquad \text{Eq. (11)}$$

$\rho_{m,T}$ is described as the density of mixtures $\rho_{1,T}$ and $\rho_{2,T}$ are the density of mono-solvents at saturated state. This trained model can predict the experimental density data with *MRD*% of 0.8%. The densities for investigated system are listed in Table 6. One can train this model by density data for NMP and ethanol system without solute,[17] to propose a predictive equation. Its advantage is that it only needs the density in the neat solvents. *MRDs*% in this state are 2.6, 2.6, 2.6, 2.4 and 1.5% for investigated temperatures with overall *MRD*% of 2.3%.

Thermodynamic studies

ΔH^o, ΔS^o, and ΔG^o were obtained using the Gibbs and van't Hoff models at T_{hm} and reported in Table 7. ΔH^o values were positive and the maximum amount (33.54 kJ.mol^{-1}) and minimum one (9.46 kJ.mol^{-1}) are in NMP

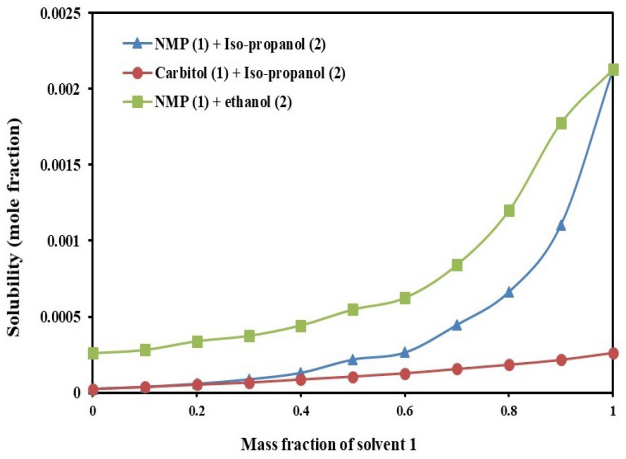

Figure 2. A comparison between present system for codeine phosphate with reported ones in the literature at 298.2 K.

Table 1. Solubility values (± standard deviation) for codeine phosphate in NMP and ethanol mixtures.

w_1[a]	293.2 K	298.2 K	303.2 K	308.2 K	313.2 K
			$X_{M,T}$ (Mole fraction)		
0.00	2.08 (±0.21) × 10^{-4}	2.60 (±0.18) × 10^{-4}	2.90 (±0.29) × 10^{-4}	3.67 (±0.49) × 10^{-4}	4.39 (±0.33) × 10^{-4}
0.10	2.52 (±0.01) × 10^{-4}	2.81 (±0.09) × 10^{-4}	3.25 (±0.45) × 10^{-4}	3.66 (±0.14) × 10^{-4}	4.10 (±0.37) × 10^{-4}
0.20	3.14 (±0.18) × 10^{-4}	3.39 (±0.21) × 10^{-4}	3.74 (±0.80) × 10^{-4}	4.05 (±0.50) × 10^{-4}	4.41 (±0.65) × 10^{-4}
0.30	3.46 (±0.13) × 10^{-4}	3.74 (±0.10) × 10^{-4}	4.12 (±0.22) × 10^{-4}	4.72 (±0.52) × 10^{-4}	5.48 (±0.27) × 10^{-4}
0.40	4.09 (±0.22) × 10^{-4}	4.43 (±0.34) × 10^{-4}	5.01 (±0.39) × 10^{-4}	5.72 (±0.13) × 10^{-4}	6.72 (±0.13) × 10^{-4}
0.50	4.53 (±0.30) × 10^{-4}	5.47 (±0.79) × 10^{-4}	6.45 (±0.28) × 10^{-4}	7.95 (±0.41) × 10^{-4}	9.28 (±0.43) × 10^{-4}
0.60	5.61 (±0.09) × 10^{-4}	6.24 (±0.03) × 10^{-4}	7.61 (±0.34) × 10^{-4}	1.06 (±0.05) × 10^{-3}	1.29 (±0.05) × 10^{-3}
0.70	7.12 (±0.33) × 10^{-4}	8.42 (±0.37) × 10^{-4}	9.56 (±0.18) × 10^{-4}	1.36 (±0.02) × 10^{-3}	1.68 (±0.09) × 10^{-3}
0.80	1.02 (±0.06) × 10^{-3}	1.20 (±0.01) × 10^{-3}	1.47 (±0.04) × 10^{-3}	1.77 (±0.28) × 10^{-3}	2.03 (±0.05) × 10^{-3}
0.90	1.61 (±0.20) × 10^{-3}	1.77 (±0.20) × 10^{-3}	1.98 (±0.15) × 10^{-3}	2.26 (±0.04) × 10^{-3}	2.51 (±0.21) × 10^{-3}
1.00	2.07 (±0.02) × 10^{-3}	2.13 (±0.10) × 10^{-3}	2.39 (±0.12) × 10^{-3}	2.50 (±0.12) × 10^{-3}	2.60 (±0.04) × 10^{-3}
			$C_{m,T}$ (mol.L^{-1})		
0.00	3.63 (±0.21) × 10^{-3}	4.53 (±0.21) × 10^{-3}	5.03 (±0.21) × 10^{-3}	6.35 (±0.21) × 10^{-3}	7.18 (±0.21) × 10^{-3}
0.10	4.28 (±0.01) × 10^{-3}	4.57 (±0.01) × 10^{-3}	5.66 (±0.01) × 10^{-3}	6.15 (±0.01) × 10^{-3}	6.85 (±0.01) × 10^{-3}
0.20	5.15 (±0.18) × 10^{-3}	5.54 (±0.18) × 10^{-3}	6.09 (±0.18) × 10^{-3}	6.59 (±0.18) × 10^{-3}	7.10 (±0.18) × 10^{-3}
0.30	5.46 (±0.13) × 10^{-3}	5.89 (±0.13) × 10^{-3}	6.47 (±0.13) × 10^{-3}	7.40 (±0.13) × 10^{-3}	8.51 (±0.13) × 10^{-3}
0.40	6.21 (±0.22) × 10^{-3}	6.69 (±0.22) × 10^{-3}	7.56 (±0.22) × 10^{-3}	8.61 (±0.22) × 10^{-3}	1.00 (±0.22) × 10^{-2}
0.50	6.57 (±0.30) × 10^{-3}	7.90 (±0.30) × 10^{-3}	9.30 (±0.30) × 10^{-3}	1.14 (±0.30) × 10^{-2}	1.32 (±0.30) × 10^{-2}
0.60	7.74 (±0.09) × 10^{-3}	8.57 (±0.09) × 10^{-3}	1.04 (±0.09) × 10^{-2}	1.45 (±0.09) × 10^{-2}	1.76 (±0.09) × 10^{-2}
0.70	9.28 (±0.33) × 10^{-3}	1.10 (±0.33) × 10^{-32}	1.24 (±0.33) × 10^{-2}	1.75 (±0.33) × 10^{-2}	2.16 (±0.33) × 10^{-2}
0.80	1.28 (±0.06) × 10^{-2}	1.46 (±0.06) × 10^{-2}	1.78 (±0.06) × 10^{-2}	2.15 (±0.06) × 10^{-2}	2.44 (±0.06) × 10^{-2}
0.90	1.83 (±0.20) × 10^{-2}	2.02 (±0.20) × 10^{-2}	2.24 (±0.20) × 10^{-2}	2.55 (±0.20) × 10^{-2}	2.98 (±0.20) × 10^{-2}
1.00	2.13 (±0.20) × 10^{-2}	2.18 (±0.20) × 10^{-2}	2.46 (±0.20) × 10^{-2}	2.59 (±0.20) × 10^{-2}	2.99 (±0.20) × 10^{-2}

[a] w_1 is mass fraction of NMP in NMP and ethanol mixtures in the absence of codeine phosphate.

mass fraction w_1 =0.6 and w_1 =1.0, respectively. ΔS^o values were positive except NMP mass fractions of w_1 =0.1 to 0.4 and w_1 =1.0 showing that the procedure is neither enthalpy - nor entropy driven in these solutions. ΔG^o values were in 9.46 - 27.60 kJ.mol^{-1} range and they decrease with an increase in NMP concntration. Minimum value was for pure NMP, which showed that dissolution procedure is more favorable in pure NMP. Moreover, *z and* values were summarized in Table 7.

ΔH^o vs ΔG^o was drawn for investigation of the cosolvency mechanism. Figure 3 gives a non-linear pattern with one region with a negative slope $0.2 \leq w_1 \leq 0.6$ illustrating an entropy-driven trend and two regions with a positive slope ($0.0 \leq w_1 \leq 0.2$ and $0.7 \leq w_1 \leq 1.0$) showing an enthalpy-driven mechanism.

Table 2. van't Hoff equation coefficients and the *MRD*% for codeine phosphate solubility in NMP and ethanol mixture.

w_1	*A*	*B*	*MRD*%
0.00	3.037	-3376.185	2.0
0.10	-0.549	-2270.290	0.5
0.20	-2.721	-1568.508	0.4
0.30	-0.801	-2110.194	2.3
0.40	-0.029	-2287.704	2.4
0.50	3.621	-3319.985	0.8
0.60	6.181	-4027.427	5.3
0.70	6.437	-4027.439	4.7
0.80	4.161	-3241.533	1.2
0.90	0.637	-2076.186	0.8
1.00	-2.308	-1137.755	1.6
Overall			2.0

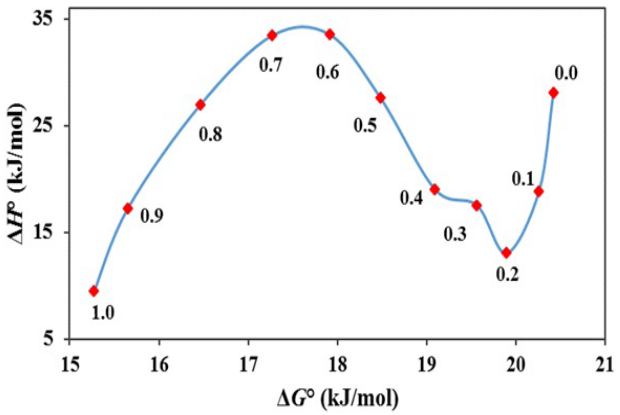

Figure 3. The plot of Enthalpy-entropy compensation for current solute in NMP and ethanol mixture at T_{hm}.

Table 3. MRS equation coefficients and *MRD*% for codeine phosphate solubility in NMP and ethanol mixture.

T (K)	β_1	β_2	β_3	β_4	β_5	*MRD*%
293.2	-6.058	-8.183	-0.006	0[a]	-2.155	4.6
298.2	-6.018	-8.254	0[a]	0[a]	-1.567	3.9
303.2	-5.74	-8.130	0[a]	-0.004	-1.78	2.8
308.2	-5.582	-8.190	-0.005	-0.007	-1.088	3.1
313.2	-5.619	-8.313	0.011	-0.006	0[a]	4.2
Overall *MRD*%						3.7

[a] Not statistically significant (*p*-value >0.05)

Table 4. Coefficients of Jouyban-Acree, and Jouyban-Acree-van't Hoff equation and *MRD*% for codeine phosphate solubility in NMP and ethanol mixture.

	Jouyban-Acree		Jouyban-Acree-van't Hoff	
	J_0	-304.230	A_1	-2.308
	J_1	232.983	B_1	-1137.755
	J_2	0[a]	A_2	3.037
			B_2	-3376.185
			J_0	-304.547
			J_1	232.472
			J_2	0[a]
MRD%	7.6		8.0	

[a] Not statistically significant (*p*-value >0.05)

Table 5. The λh model parameters and *MRD*% for codeine phosphate solubility in NMP and ethanol mixture.

w_1	*l*	*h*	*MRD*%
0.00	0.501	4.193	3.8
0.10	0.501	2.959	1.5
0.20	0.501	2.354	0.8
0.30	0.500	3.692	3.4
0.40	0.501	4.824	3.6
0.50	0.502	8.828	2.7
0.60	0.503	13.950	8.4
0.70	0.503	18.060	7.9
0.80	0.504	19.049	2.6
0.90	0.504	16.805	1.6
1.00	0.503	10.569	1.5
Overall			3.4

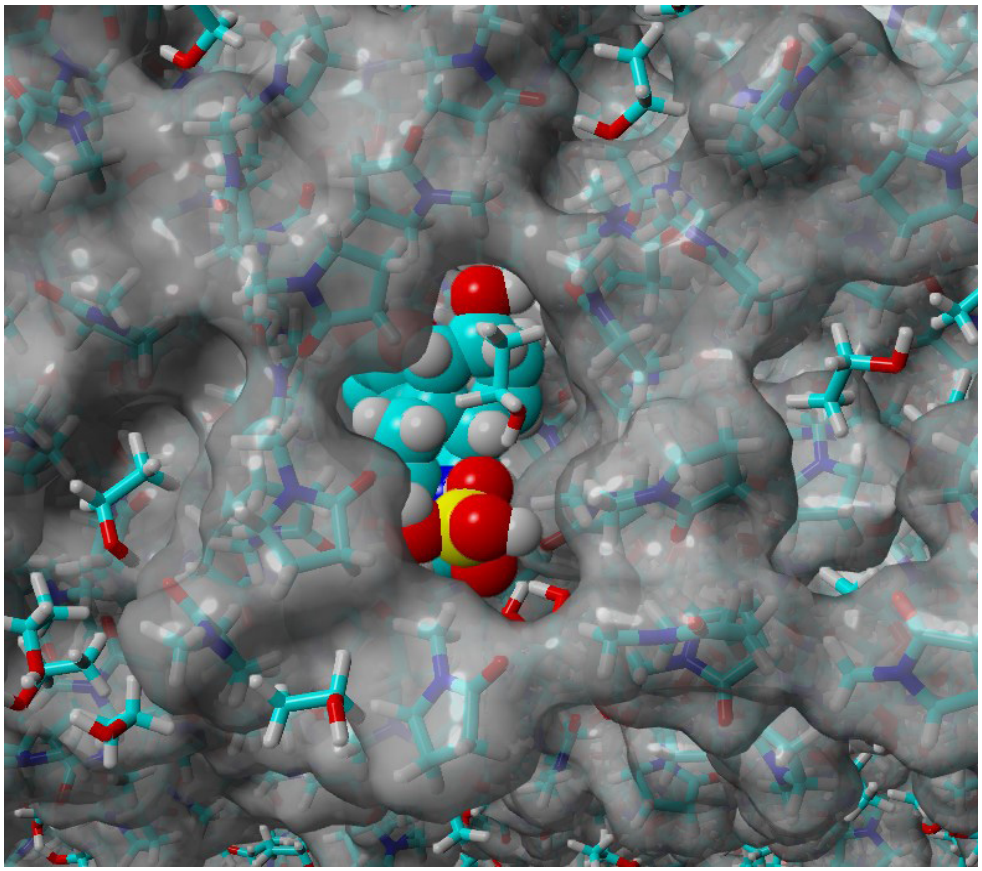

Figure 4. Schematic illustration of a molecular dynamics simulation (5 ns) showing codeine phosphate as space-filled model, whereas the solvents are given as in tubes. The molecular surface is shown for NMP to better graphical discrimination the different solvents. Details are given in the text.

Table 6. Density (g.cm^{-3}) of investigated mixtures at various temperatures.

w_1	293.2 K	298.2 K	303.2 K	308.2 K	313.2 K
0.00	0.807 ± 0.001	0.803 ± 0.001	0.801 ± 0.001	0.799 ± 0.001	0.795 ± 0.010
0.10	0.826 ±0.001	0.823 ± 0.001	0.821 ± 0.001	0.819 ± 0.001	0.814 ± 0.001
0.20	0.847 ± 0.001	0.844 ± 0.001	0.842 ± 0.001	0.841 ± 0.010	0.833 ± 0.001
0.30	0.869 ± 0.001	0.865 ± 0.001	0.864 ± 0.001	0.863 ± 0.010	0.855 ± 0.001
0.40	0.891 ± 0.001	0.887 ± 0.001	0.886 ± 0.001	0.884 ± 0.010	0.877 ± 0.001
0.50	0.913 ± 0.001	0.909 ± 0.001	0.909 ± 0.001	0.908 ± 0.001	0.900 ± 0.001
0.60	0.938 ± 0.001	0.934 ± 0.001	0.934 ± 0.001	0.930 ± 0.001	0.927 ± 0.001
0.70	0.962 ± 0.001	0.961 ± 0.001	0.958 ± 0.001	0.956 ± 0.001	0.950 ± 0.001
0.80	1.014 ± 0.001	0.984 ± 0.001	0.983 ± 0.001	0.983 ± 0.001	0.976 ± 0.001
0.90	1.015 ± 0.010	1.014 ± 0.010	1.011 ± 0.001	1.007 ± 0.001	1.005 ± 0.001
1.00	1.028 ± 0.001	1.024 ± 0.001	1.023± 0.010	1.020 ± 0.010	1.020 ± 0.001

Table 7. Thermodynamic factors for dissolution of codeine phosphate in NMP and ethanol mixtures at T_{hm}.

w_1	ΔG° (kJ.mol^{-1})	ΔH° (kJ.mol^{-1})	ΔS° (J.K^{-1}.mol^{-1})	TΔS° (kJ.mol^{-1})	ζH	ζTs
0.00	20.42	28.07	25.24	7.65	0.786	0.214
0.10	20.26	18.88	-4.54	-1.38	0.932	0.068
0.20	19.89	13.05	-22.59	-6.85	0.656	0.344
0.30	19.56	17.54	-6.69	-2.03	0.896	0.104
0.40	19.09	19.02	-0.228	-0.07	0.996	0.004
0.50	18.48	27.60	30.09	9.12	0.752	0.248
0.60	17.91	33.54	51.56	15.62	0.682	0.318
0.70	17.27	33.44	53.38	16.17	0.674	0.326
0.80	16.47	26.98	34.70	10.52	0.720	0.280
0.90	15.65	17.28	5.38	1.63	0.914	0.086
1.00	15.27	9.46	-19.19	-5.81	0.619	0.381

Atomistic simulation of a solvent mixture

An MD simulation at w_1 = 0.5 solvent mixture was conducted to visualize the solvation process of codeine phosphate. Figure 4 depicts a snapshot after 5 ns simulation time with codeine phosphate as space filled model and the solvent molecules shown as tubes. For better discrimination of individual solvent effects, the molecular surface of NMP is shown. As expected, the ion pair of protonated codeine and dihydrogen phosphate stayed together in the non-aqueous solvation environment. The MD simulation suggested a pronounced contribution of hydrogen boding to solvation, whereby both solvents acted as hydrogen bond acceptors, but ethanol was further able to donate hydrogen bonds. However, this is only a qualitative differentiation and in terms of overall solvation effects, there appeared to be some preferential solvation by NMP, which reflects the high solubilizing potency of this solvent that was observed experimentally.

Conclusion

Herein, the experimental data for codeine phosphate in NMP and ethanol system at five temperatures in the range of 293.2 – 313.2 K were obtained and fitted to the some cosolvency equations including van't Hoff, MRS, the Jouyban-Acree, the Jouyban-Acree-van't Hoff and λh equations. Moreover, accuracy of the equations was investigated by obtaining *MRDs*% which for the investigated models were <8.0% demonstrating the excellent solubility prediction capability of these models. Moreover, the thermodynamic factors for codeine phosphate in NMP and ethanol system were also calculated by Gibbs and van't Hoff models. Results showed that codeine phosphate solubility procedure was endothermic and thermodynamically favorable in high NMP concentration with low free Gibbs energy in this solvent.

Author Contributions

Homa Rezaei: Investigation, Formal Analysis. Martin Kuentz: Methodology, Writing - Review & Editing. Hongkun Zhao: Data visualizing, Writing - Review & Editing. Elaheh Rahimpour: Methodology, Supervision, Writing - Original Draft. Abolghasem Jouyban: Conceptualization, Writing - Review & Editing.

Acknowledgements

This research was supported by the Student Research Committee with grant number 67435 Tabriz University of Medical Sciences, Tabriz, Iran.

Conflict of Interest

The authors declare that they have no competing interests.

Supplementary Data

Supplementary data, Table S1, are available at https://doi.org/10.34172/PS.2023.2.

References

1. Dahan A, Wolk O, Zur M, Amidon GL, Abrahamsson B, Cristofoletti R, et al. Biowaiver monographs for immediate-release solid oral dosage forms: Codeine phosphate. J Pharm Sci. 2014;103(6):1592-600. doi:10.1002/jps.23977
2. Mandal SC, Mandal V, Das AK. Essentials of botanical extraction: Principles and Applications. Cambridge, Massachusetts: Academic press; 2015.
3. Swarbrick J, Boylan JC. Encyclopedia of pharmaceutical technology. Volume 1. New York: Marcel Dekker; 2007.
4. Yalkowsky SH. Solubility and solubilization in aqueous media: New York: American Chemical Society and Oxford University Press; 1999.
5. Strickley RG. Solubilizing excipients in oral and injectable formulations. Pharm Res. 2004;21(2):201-30. doi:10.1023/b:pham.0000016235.32639.23
6. Jouyban A, Fakhree MAA, Shayanfar A. Review of pharmaceutical applications of N-methyl-2-pyrrolidone. J Pharm Pharm Sci. 2010;13(4):524-35. doi:10.18433/J3P306
7. Lee PJ, Langer R, Shastri VP. Role of n-methyl pyrrolidone in the enhancement of aqueous phase transdermal transport. J Pharm Sci. 2005;94(4):912-7. doi:10.1002/jps.20291
8. Benita S. Microencapsulation: Methods and industrial applications. New York: CRC Press; 2005.
9. Jouyban-Gharamaleki A. The modified wilson model and predicting drug solubility in water-cosolvent mixtures. Chem Pharm Bull. 1998;46(6):1058-61. doi:10.1248/cpb.46.1058
10. Vahdati S, Shayanfar A, Hanaee J, Martínez F, Acree Jr. WE, Jouyban A. Solubility of carvedilol in ethanol+ propylene glycol mixtures at various temperatures. Ind Eng Chem Res. 2013;52(47):16630-36. doi:10.1021/ie403054z
11. Tinjacá DA, Martínez F, Almanza OA, Jouyban A, Acree WE. Solubility, correlation, dissolution thermodynamics and preferential solvation of meloxicam in aqueous mixtures of 2-propanol. Pharm Sci. 2022;28(1):130-44. doi:10.34172/PS.2021.39
12. Jafari P, Rahimpour E, Jouyban A. Solubility of bosentan in polyethylene glycol 400+ water mixtures: experimental and mathematical computations. Pharm Sci. 2023;29(2):228-35. doi:10.34172/PS.2022.13
13. Perlovich GL, Kurkov SV, Bauer-brandl A. Thermodynamics of solutions: II. Flurbiprofen and diflunisal as models for studying solvation of drug substances. Eur J Pharm Sci. 2003;19:423-32. doi:10.1016/S0928-0987(03)00145-3
14. Krieger E, Vriend G. YASARA View - molecular graphics for all devices - from smartphones to workstations. Bioinformatics. 2014;30(20):2981-2. doi:10.1093/bioinformatics/btu426
15. Essmann U, Perera L, Berkowitz ML, Darden T, Lee H, Pedersen LG. A smooth particle mesh ewald method. J Chem Phys. 1995;103(19):8577-93. doi:10.1063/1.470117
16. Jakalian A, Jack DB, Bayly CI. Fast, efficient generation of high-quality atomic charges. AM1-BCC model: II. Parameterization and validation. J Comput Chem. 2002;23(16):1623-41. doi:10.1002/jcc.10128
17. García-Abuín A, Gomez-Diaz D, La Rubia M, Navaza J. Density, speed of sound, viscosity, refractive index, and excess volume of n-methyl-2-pyrrolidone+ ethanol (or water or ethanolamine) from t=(293.15 to 323.15) k. J Chem Eng Data. 2011;56(3):646-51. doi:10.1021/je100967k